JOURNAL OF SOLID STATE CHEMISTRY 63, 110–117 (1986)

Crystallography and Optical Energy Gap Values for $Cd_{2x}(CuIn)_yMn_{2z}Te_2$ Alloys

MIGUEL QUINTERO,* LAURA DIERKER, AND JOHN C. WOOLLEY

Physics Department, University of Ottawa, Ottawa, Ontario K1N 6N5, Canada

Received August 23, 1985; in revised form November 1, 1985

Polycrystalline samples of $Cd_{2x}(CuIn)_yMn_{2z}Te_2$ ($x + y + z = 1$) alloys were prepared by a melt and anneal technique. Debye-Scherrer X-ray powder photographs were used to determine equilibrium conditions and lattice parameter values. It was found that in addition to the zinc blende and chalcopyrite structures, a partially ordered cubic structure was obtained, plus a two-phase field at higher z values. Room-temperature measurements of optical absorption were made to give values of the optical energy gap E_g for all single phase samples. It was found that the variation of a was practically linear with composition and so could not be used to determine the boundaries between the three different phase fields. However, while E_g varied linearly with composition inside a phase field, the resulting lines had different aiming points at $z = 1$, the values being 2.83 eV for zinc blende, 1.90 eV for the ordered cubic phase, and 1.36 eV for the chalcopyrite phase. Thus the values of E_g give a very good indication of the phase boundaries.

Introduction

The names semimagnetic semiconductor alloy or diluted magnetic semiconductor have been applied to materials obtained by substituting, at random, a paramagnetic ion on the cation sublattice of a compound semiconductor. These materials have been the subject of various investigations because the presence of this paramagnetic ion causes differences in the semiconducting behavior, particularly in a magnetic field, from that of normal semiconductor and also introduces interesting magnetic behavior. If the alloy to be produced is to be a semiconductor, then the electron to atom ratio must be conserved; i.e., on the average, the magnetic ions must replace nonmagnetic cations of the same valency.

Most of the work (*1–4*) on such alloys has been carried out on alloys involving divalent manganese in pseudo-binary systems of the type $Cd_{1-z}Mn_zTe$, $Hg_{1-z}Mn_zTe$, $Cd_{1-z}Mn_zSe$, etc. Recently, this work has been extended to pseudo-ternary alloy systems such as $Cd_xHg_yMn_zTe$ (*5*) and $Cd_xZn_yMn_zTe$ (*6–8*) with $x + y + z = 1$.

Other possible semimagnetic alloys can be derived from the chalcopyrite I III VI_2 compounds, the ternary analogs of the II VI compounds. Some work has been carried out with alloys in which Fe^{3+} ions replace III cations in the chalcopyrite lattice, e.g., $Cu(Al_{1-z}Fe_z)S_2$ (*9*), etc. However, no work has been published so far on the inclusion of Mn^{2+} in a chalcopyrite material. To retain the electron to atom ratio, it is neces-

* On leave from Universidad de los Andes, Merida, Venezuela.

0022-4596/86 $3.00

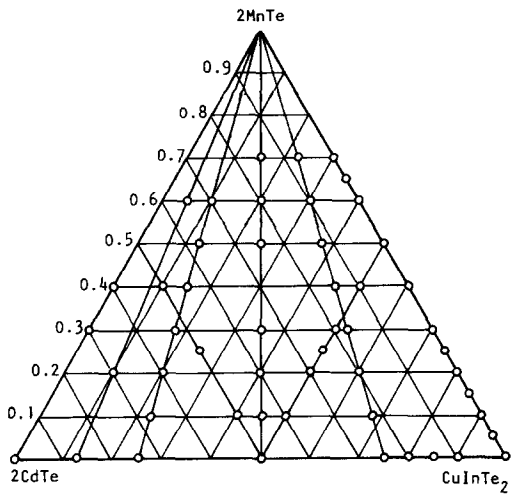

FIG. 1. Composition diagram showing samples used in this work.

sary in this case to replace one I and one III cation simultaneously by two manganese atoms. Thus in the present work, the alloy system $(CuIn)_{1-z}Mn_{2z}Te_2$ has been investigated.

Previous work has shown that a wide range of solid solution can usually be obtained between a I III VI_2 compound and its II VI binary analog, e.g., $Cd_{2(1-y)}(CuIn)_yS_2$ (*10*), $Cd_{2(1-y)}(AgIn)_yTe_2$ and $Cd_{2(1-y)}(CuGa)_yTe_2$ (*11*). In the case of $Cd_{2(1-y)}(CuIn)_yTe_2$, Chernyavsky (*12*) reported single phase solid solution across the whole composition range but gave no values of lattice parameter and no values of other physical parameters for these alloys have been given in the literature. In the present work, the study of the chalcopyrite alloys has been extended to the pseudo-ternary system $Cd_{2x}(CuIn)_yMn_{2z}Te_2$ ($x + y + z = 1$).

Preparation of Samples and Methods of Measurements

The initial requirement of any investigations of alloy systems of this type is to determine the composition range over which single phase solid solution occurs and hence this was the first work carried out in the present program. To facilitate comparison of results, samples were made at compositions along the lines in the phase diagram at constant $x : y$ ratio, i.e., $y = 0$, $x = 7y$, $x = 3y$, $x = y$, $3x = y$, and $x = 0$, and at various fixed values of z as shown in Fig. 1. Samples along the line $y = 0.5$ were also investigated in some detail. For each alloy composition chosen, a 1-g polycrystalline sample was made up from the elements by the standard melt and anneal technique. In each case, the appropriate weights of the elements were sealed under vacuum in a quartz tube which had previously been carbonized. The carbonizing of the tube was found necessary to reduce the interaction of the alloy with the quartz at the higher temperatures. The sample was then heated to 1150°C, at which temperature all components of the alloy were melted except the manganese, and this reacted with or dissolved in the melt. The melt was left at 1150°C for at least half an hour to homogenize and was then cooled to room temperature. The sealed sample was then placed to anneal at 600°C. After annealing, Debye–Scherrer powder X-ray photographs were used to check the conditions of each annealed sample and to determine whether a single phase form was obtained. It was found that an annealing period of from 20 to 30 days produced good equilibrium conditions.

The initial measurement of the semiconductor properties of the alloys was to determine values of room-temperature energy gap using the optical absorption method described previously (*13*). For each sample found to be single phase, slices were cut from the ingot and polished down to thickness (d) in the range 50–150 μm. These were then used for standard transmission measurements. The variation of I_0, the incident intensity, and I_t, the transmitted inten-

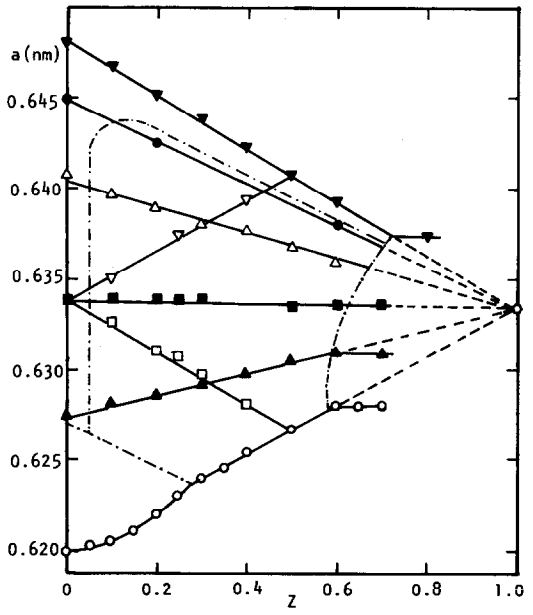

FIG. 2. Variation of lattice parameter a with z for various $x:y$ ratios. (○) $x = 0$, (▲) $y = 3x$, (■) $y = x$, (△) $x = 3y$, (●) $x = 7y$, (▼) $y = 0$, (□) $y = 0.5$, (▽) $x = 0.5$. (–·–·) Phase boundary.

sity, as a function of photon energy $h\nu$ were determined as a continuous curve on a chart recorder. Thus values of the ratio I_0/I_t were determined also as a continuous function of $h\nu$. The values of $1/d \ln I_0/I_t$ were corrected by subtracting a background value so as to give values of the absorption coefficient α. The relation $\alpha h\nu = A(E_g - h\nu)^{1/n}$ was then used to give a value for the optical energy gap E_g.

Phase Diagram and Lattice Parameter Results

It was found that all of the single phase samples gave X-ray photographs which appeared to show the zinc blende structure typical of CdTe. For each, a value of the lattice parameter a was determined and these values are shown plotted as a function of z for constant $x:y$ ratio in Fig. 2, and as a function of y at constant z in Fig. 3. At high z values, lines of the nickel arsenide structure of MnTe were observed in addition to the apparent zinc blende lines. Values of the zinc blende a parameter were determined for these two phase samples and these also are shown in Fig. 2. The slope discontinuities in the graphs of a vs z at constant $x:y$ ratio gave the limits of single phase behavior shown in Fig. 4. The lines of a vs z in the single phase range appeared to be linear within the limits of experimental error except for the case of the $x = 0$ line at low z, i.e., close to $CuInTe_2$. The graphs of a vs y are linear in the range $0.2 < y < 0.75$ but may show some curvature for $0 < y < 0.2$ while for $0.75 < y < 1.0$ there is appreciable curvature. These effects will be discussed below.

As is seen from Fig. 2, if the a vs z lines in the single phase range are extrapolated to $z = 1.0$, they coincide at a value of $a = 0.6333$ nm which represents the value of a that MnTe would have in the zine blende structure. This is in good agreement with the equivalent value obtained for the $Cd_xZn_yMn_zTe$ alloys (7).

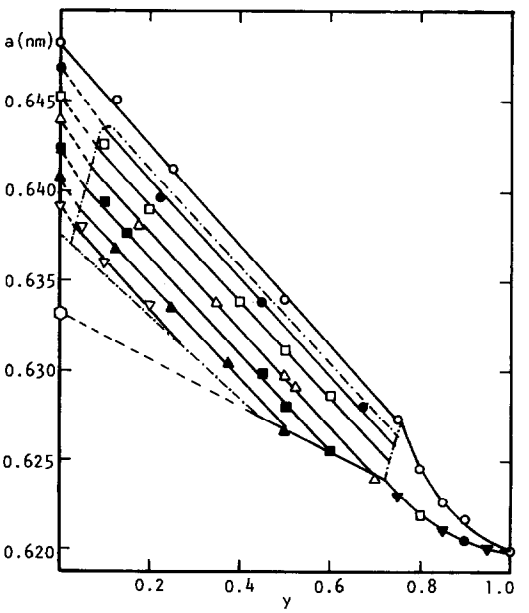

FIG. 3. Variation of lattice parameter a with y for various constant values of z. z: (○) 0.0, (●) 0.1, (□) 0.2, (△) 0.3, (■) 0.4, (▲) 0.5, (▽) 0.6; (▼) $x = 0$. (–·–·) Phase boundary.

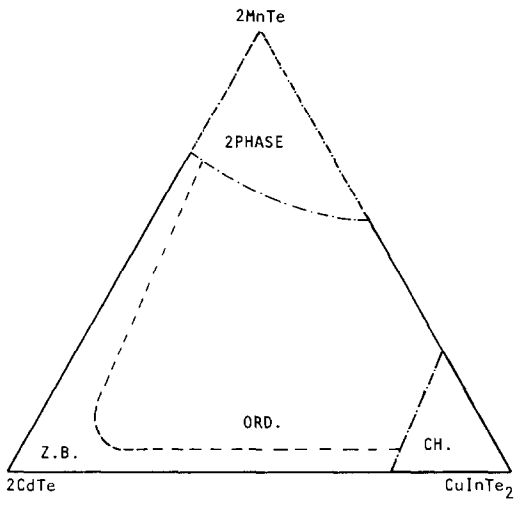

FIG. 4. Isothermal section showing phase boundaries.

For interpolation purposes, this linear variation of a with composition was fitted to an equation linear in y and z, giving

$$a = 0.6475 - 0.0260y - 0.0142z \text{ nm}$$

with standard deviation of the fitted points of $\sigma = 0.0002$ nm.

As is well known (*14*), $CuInTe_2$ is tetragonal with $c/a = 2$ and so gives the pseudocubic result indicated above. However, relatively faint ordering lines could be observed in the X-ray photographs for $CuInTe_2$ and alloys close in composition to this. Observation of these lines was used to give an estimate of the boundary of the chalcopyrite ordered phase indicated in Fig. 4. Because the intensity of these ordering lines was reduced as the composition was moved away from $CuInTe_2$, the accuracy of this estimate was not good. Another possible indication of the range of chalcopyrite structure is given by the variation of a with composition on the $z = 0$ and $y = 0$ edges (Figs. 2 and 3) since changes in slope occur in the graphs of a vs composition. However, a linear variation of a with composition might be expected inside the ordered phase field, whereas a distinct curvature is observed. One possibility is that there is a change in the degree of order as the composition varies away from $CuInTe_2$. However, another factor of interest is one of nonstoichiometry. The value of a for $CuInTe_2$ has been reported at values from 0.618 to 0.616 nm (*14*) and the difference attributed to small changes in stoichiometry of the compound. Here a value of 0.620 nm has been obtained, with corresponding values for the adjacent alloy compositions. It appears probable that the curvature of the a vs y and a vs z curves can be attributed to a systematic variation in stoichiometry for alloys produced by the melt and anneal technique. Thus although the values of a give some indication of the range of ordering, it is of interest to obtain further information and, as indicated below, this is given by the optical energy gap data.

Study of the X-ray photographs showed that over some of the single phase field, faint lines were observed indicating the presence of an ordering different from that of the chalcopyrite structure. In this case, the ordering lines showed maximum intensity in the range $z \sim 0.20$ to 0.25 and the intensity fell off progressively as z was increased or decreased from this value. The structure of this ordered phase has not as yet been fully determined. As indicated above, the variation of the parameter a with z was linear within the limits of experimental error and hence would not show the boundary of this partially ordered structure. In the case of the a vs y graphs, the small curvature at low y values, i.e., in the vicinity of the $Cd_{1-z}Mn_zTe$ line, may be due to a change from ordered to disordered structure, but no good estimate of the boundary of the ordered phase could be obtained from these data. Because of the low intensity of the ordering lines, the boundary could not be obtained with any accuracy from intensity measurements either. However, once again, as indicated below, the values of energy gap were found to give a

good indication of the range in which this partial ordering occurred.

Energy Gap Results and Analysis

It is established that both CdTe and $CuInTe_2$ are direct band gap semiconductors and previous work (*7*) has shown that all alloys along the $y = 0$ edge ($Cd_{1-z}Mn_zTe$) also have direct gaps. A direct allowed transition requires $n = 2$ (*16*) and hence initially all of the optical absorption data were analyzed using $n = 2$, i.e., graphs of $(\alpha h\nu)^2$ plotted against $h\nu$. It was found over much of the alloy range that these graphs showed some deviation from linearity and that plots with $n = \frac{1}{2}$ (indirect gap) or $n = \frac{2}{3}$ (forbidden direct gap) give curves nearer to straight lines over the range of α which could be determined with the present samples. A case for which this is very noticeable is shown in Fig. 5. The range of α was limited because with the polycrystalline material used, it was not possible to polish samples down below a certain thickness before they disintegrated. These graphs of $(\alpha h\nu)^n$ vs $h\nu$ raised the question of whether the partially ordered samples showed a different band gap behavior from the CdTe alloys.

The possibility of indirect gap behavior has been raised in the past over some of the chalcopyrite compounds. Thus in the case of $CuInTe_2$, from photovoltaic measurements Parkes *et al.* (*17*) suggested that the results were typical of indirect gap behavior, i.e., with $n = \frac{1}{2}$. However, detailed study of various I III VI_2 compounds (*14*) led to the conclusion that these have a direct gap at the Γ point. The possibility of a forbidden direct gap with $n = \frac{2}{3}$ initially appeared feasible because in these alloys there is an appreciable admixture of *d* character in the valence band (e.g., (*9, 18*)). However, theoretical analysis (*15*) shows that for transitions at the Γ point, the value

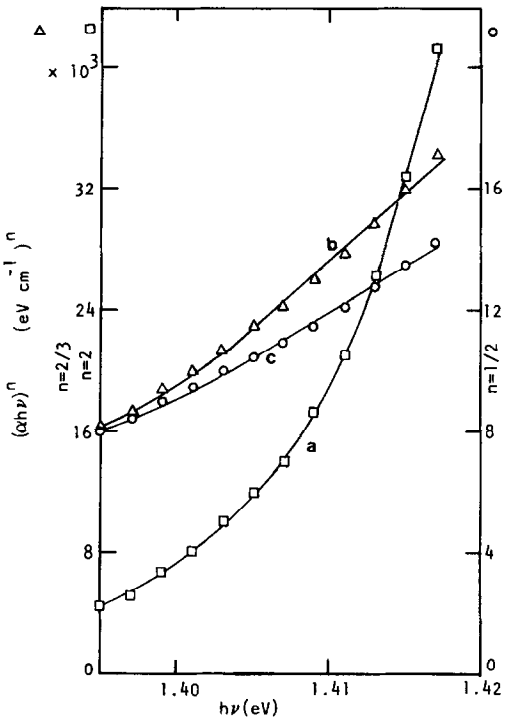

FIG. 5. Variation of $(\alpha h\nu)^n$ with $h\nu$ for sample with $y = 0.375$, $z = 0.5$; (a) $n = 2$, (b) $n = (\frac{2}{3})$, (c) $n = (\frac{1}{2})$.

of α for allowed transitions would be very much larger than for forbidden, so that even when the valence band has appreciable *d* character, the α contribution of the allowed transition from the *p* character of the valence band would predominate. Thus it appears probable that for all of these alloys the band gap is direct and that the nonlinearity of the $(\alpha h\nu)^2$ vs $h\nu$ graph at lower values of α is due to some other effect. One possible effect is the band tailing which occurs to some extent in randomly substituted alloys (*19*). However, perhaps a more important effect is the tailing of the direct gap absorption edge due to transitions involving optical phonons which occur below the direct gap value (*16*). In the case of $CuInSe_2$, Rincon *et al.* (*20*) have observed such transitions in detailed optical absorption measurements at low temperatures. Tailing of

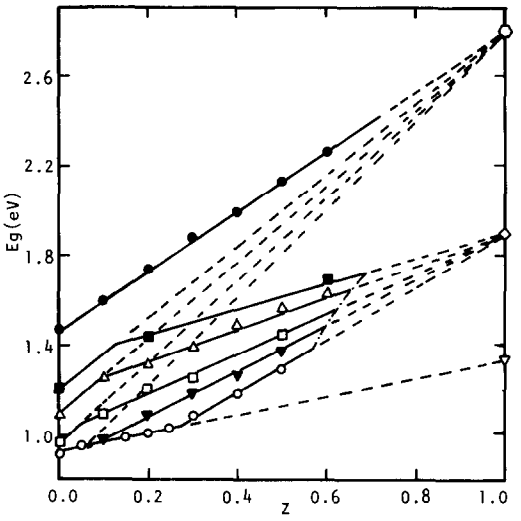

FIG. 6. Variation of room-temperature energy gap E_g with z for various $x:y$ ratios. (○) $x = 0$, (▼) $y = 3x$, (□) $y = x$, (△) $x = 3y$, (■) $x = 7y$, (●) $y = 0$.

the absorption can also be produced by large impurity concentrations in a semiconductor.

Therefore in the present work, plots of $(\alpha h\nu)^2$ vs $h\nu$ have been used throughout to determine energy gap values, the high values of $(\alpha h\nu)^2$ being extrapolated to give E_g. Thus, for example, in Fig. 5 the higher values of α on the $(\alpha h\nu)^2$ vs $h\nu$ curve (curve a) are seen to extrapolate to a value of E_g = 1.405 eV with an error in the extrapolation of less than ± 5 meV. It should be remembered that, as indicated above, Fig. 5 shows one of the worst curves as far as the variation of $(\alpha h\nu)^2$ with $h\nu$ is concerned. When the lines for $n = \frac{2}{3}$ were used it was found that there was a systematic reduction of 20 to 30 meV in the value of E_g as compared with the $n = 2$ case. Thus the general form and variation of the curves of E_g versus composition were practically unaffected by the criterion used to determine the E_g values.

The variation of E_g with z for various lines of constant $x:y$ ratio is shown in Fig. 6 and of E_g with x for various z values in Fig. 7. The discussion above indicates that these values of E_g should certainly not be in error by more than 20 meV. The points shown in Figs. 6 and 7 have a size a little larger than this. Thus any experimental scatter in these points is more likely due to small errors in z rather than in E_g. From Fig. 6 it is seen, as reported previously (7), that for $y = 0$ (zinc blende structure) E_g varies linearly with z and extrapolates at $z = 1$ to a value of 2.83 eV, corresponding to the value for MnTe in the zinc blende structure. For the values of $x:y$ inside the composition triangle, again linear behavior is obtained for $z > 0.1$ but the aiming point at $z = 1$ in these cases is 1.90 eV. This is thus the extrapolated value of E_g for MnTe with the ordered cubic structure. Finally, for $x = 0$ and $z < 0.3$, i.e, the chalcopyrite field, the values of E_g extrapolate at $z = 1$ to $E_g = 1.36$ eV. It is clear that the aiming point of the E_g vs z lines varies with the structure concerned and this fact can be used to determine the boundaries of the various fields. Thus in Fig. 6, each value of E_g on the $z = 0$ line has been joined to the zinc blende value of 2.83 eV at

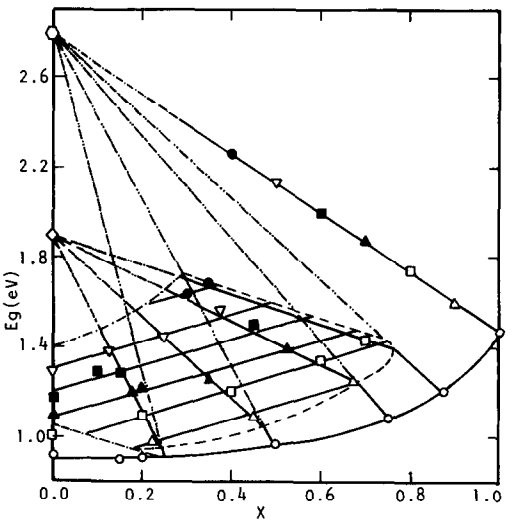

FIG. 7. Variation of room-temperature energy gap E_g with x for various constant values of z. z: (○) 0.0, (△) 0.1, (□) 0.2, (▲) 0.3, (■) 0.4. (–·–·) Phase boundaries.

$z = 1$ and the points of intersection of these lines with the corresponding ones through the experimental values for $z > 0.1$ give the boundary between the zinc blende and the ordered cubic fields. A similar construction has been carried out in Fig. 7 to give an estimate of the boundary which runs almost parallel with the $x:y = 7$ line (Figs. 1 and 4). The positions of these boundaries and also that for the chalcopyrite field are shown in Figs. 4 and 7.

Conclusions

The results obtained here show that it is possible to substitute Mn into the $CuInTe_2$ lattice and retain semiconductor properties provided that equal numbers of Cu and In atoms are simultaneously replaced by Mn. The range of solid solubility in the $(CuIn)_{1-z}Mn_{2z}Te_2$ system is found to be up to $z = 0.57$, although the chalcopyrite structure is retained only up to $z \sim 0.27$. Further, because of the single phase solid solution over the complete composition range of the $Cd_{2(1-y)}(CuIn)_yTe_2$, it is possible to obtain a wide range of single phase behavior in the pseudo-ternary system $Cd_{2x}(CuIn)_yMn_{2z}Te_2$ $(x + y + z = 1)$.

In the range of single phase behavior, there is a normal zinc blende field in which the Mn atoms substitute for nonmagnetic cations in a random manner, a field in which the chalcopyrite structure occurs again probably with random substitution on cation sites, and third, a large field in which the Mn atoms tend to order on the cation sublattice producing a structure which is still cubic. All of these phases are semiconductors and it is found that the value of the optical energy gap E_g and its variation with composition depend upon the structure concerned. This result can be used to delineate the boundaries between the three fields. The different energy gaps have been taken in every case to be direct and it is hoped to use the values obtained in the partially ordered cubic field to give some indication of the band structure variation which occurs on ordering.

All of the alloys produced have Mn distributed through the cation sublattice and so show behavior typical of a semimagnetic semiconductor. However, while for the zinc blende and chalcopyrite cases the Mn atoms are distributed at random on the cation sublattice, for most of the alloys the Mn atoms are partially ordered on the lattice. This changes the magnetic behavior of the alloys to some extent compared with that of alloys with completely random distribution. This magnetic behavior will be discussed elsewhere.

References

1. J. K. Furdyna, *J. Appl. Phys.* **53,** 7637 (1982).
2. J. A. Gaj, *J. Phys. Soc. Japan* **49,** 797 (1980).
3. R. R. Galazka, *Inst. Phys. Conf. Ser.* **43,** 133 (1979).
4. J. Mycielski, *Progr. Cryst. Growth Charact.* **10,** 101 (1985).
5. U. Debska, M. Dietl, G. Grabecki, E. Janik, E. Kierzed-Pecold, and M. Klimkiewitz, *Phys. Status Solidi A* **64,** 707 (1981).
6. A. Manoogian, B. W. Chan, R. Brun del Re, T. Donofrio, and J. C. Woolley, *J. Appl. Phys.* **53,** 8934 (1982).
7. R. Brun del Re, T. Donofrio, J. Avon, J. Majid, and J. C. Woolley, *Il Nuovo Cimento* **2D,** 1911 (1983).
8. T. Donofrio, G. Lamarche, and J. C. Woolley, *J. Appl. Phys.* **57,** 1937 (1985).
9. T. Teranishi, K. Sato, and Y. Saito, *Inst. Phys. Conf. Ser.* **35,** 59 (1977).
10. M. Robbins, J. C. Phillips, and V. G. Lambrecht, Jr., *J. Solid State Chem.* **15,** 167 (1975).
11. J. C. Woolley and E. W. Williams, *J. Electrochem. Soc.* **113,** 849 (1966).
12. See N. A. Goryunova, "Chemistry of Diamond-like Semiconductor," p. 151, MIT Press, Cambridge, Mass., 1965.
13. R. G. Goodchild, O. H. Hughes, S. A. Lopez-Riviera, and J. C. Woolley, *Can. J. Phys.* **60,** 1096 (1982).
14. J. L. Shay and J. H. Wernick, "Ternary Chalcopyrite Semiconductors," pp. 4, 110, Pergamon, New York, 1975.
15. L. Dierker and J. C. Woolley, to be published.

16. E. J. JOHNSON, "Semimetals and Semiconductors" (R. K. Willardson and A. C. Beer, Eds.), Vol. 3, p. 153, Methuen, New York, 1967.
17. J. PARKES, R. D. TOMLINSON, AND M. J. HAMPSHIRE, *Solid State Electron.* **16,** 773 (1973).
18. P. OELHAFEN, M. P. VECCHI, J. L. FREEOUF, AND V. L. MORUZZI, *Solid State Commun.* **44,** 1547 (1982).
19. R. H. PARMENTER, *Phys. Rev.* **99,** 1759 (1955).
20. C. RINCON, J. GONZALEZ, G. SANCHEZ PEREZ, AND C. BELLABARBA, *Il Nuovo Cimento* **2D,** 1895 (1983).